

# Chapter 2

## Coordinate Systems and Transformations

### 2.1 Introduction

In navigation, guidance, and control of an aircraft or rotorcraft, there are several coordinate systems (or frames) intensively used in design and analysis (see, e.g., [171]). For ease of references, we summarize in this chapter the coordinate systems adopted in our work, which include

1. the geodetic coordinate system,
2. the earth-centered earth-fixed (ECEF) coordinate system,
3. the local north-east-down (NED) coordinate system,
4. the vehicle-carried NED coordinate system, and
5. the body coordinate system.

The relationships among these coordinate systems, i.e., the coordinate transformations, are also introduced.

We need to point out that miniature UAV rotorcraft are normally utilized at low speeds in small regions, due to their inherent mechanical design and power limitation. This is crucial to some simplifications made in the coordinate transformation (e.g., omitting unimportant items in the transformation between the local NED frame and the body frame). For the same reason, partial transformation relationships provided in this chapter are not suitable for describing flight situations on the oblate rotating earth.

### 2.2 Coordinate Systems

Shown in Figs. 2.1 and 2.2 are graphical interpretations of the coordinate systems mentioned above, which are to be used in sensor fusion, flight dynamics modeling, flight navigation, and control. The detailed description and definition of each of these coordinate systems are given next.

**Fig. 2.1** Geodetic, ECEF, and local NED coordinate systems

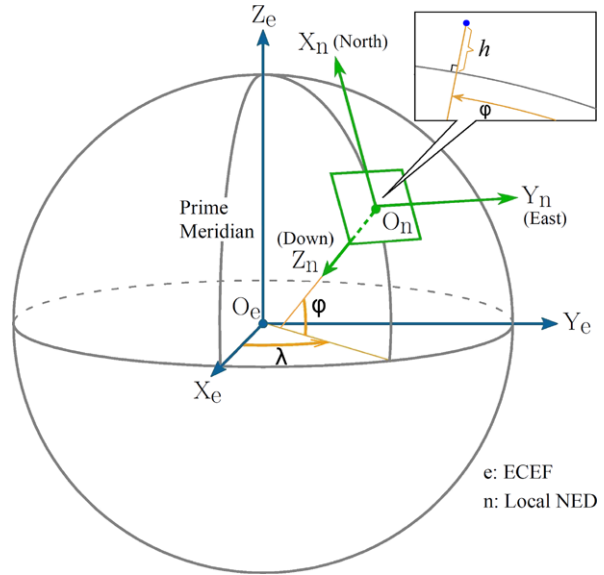
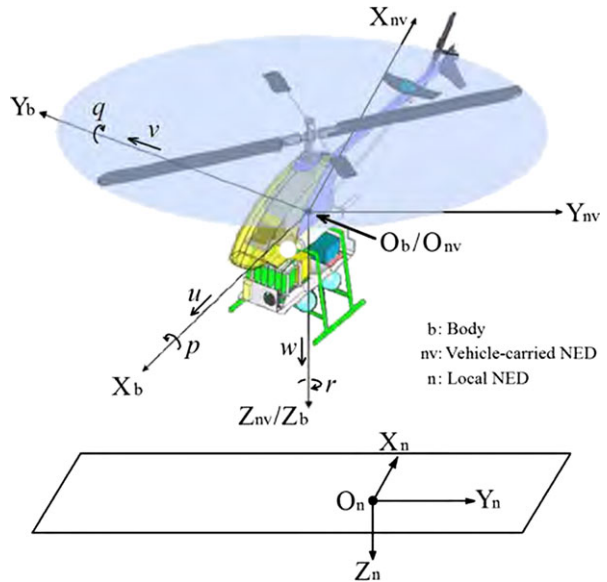


**Fig. 2.2** Local NED, vehicle-carried NED, and body coordinate systems



### 2.2.1 Geodetic Coordinate System

The geodetic coordinate system (see Fig. 2.1) is widely used in GPS-based navigation. We note that it is not a usual Cartesian coordinate system but a system that characterizes a coordinate point near the earth’s surface in terms of longitude, latitude, and height (or altitude), which are respectively denoted by  $\lambda$ ,  $\phi$ , and  $h$ . The

longitude measures the rotational angle (ranging from  $-180^\circ$  to  $180^\circ$ ) between the Prime Meridian and the measured point. The latitude measures the angle (ranging from  $-90^\circ$  to  $90^\circ$ ) between the equatorial plane and the normal of the reference ellipsoid that passes through the measured point. The height (or altitude) is the local vertical distance between the measured point and the reference ellipsoid. It should be noted that the adopted geodetic latitude differs from the usual geocentric latitude ( $\varphi'$ ), which is the angle between the equatorial plane and a line from the mass center of the earth. Lastly, we note that the geocentric latitude is not used in our work. Coordinate vectors expressed in terms of the geodetic frame are denoted with a subscript g, i.e., the position vector in the geodetic coordinate system is denoted by

$$P_g = \begin{pmatrix} \lambda \\ \varphi \\ h \end{pmatrix}. \quad (2.1)$$

Important parameters associated with the geodetic frame include

1. the semi-major axis  $R_{\text{Ea}}$ ,
2. the flattening factor  $\mathbf{f}$ ,
3. the semi-minor axis  $R_{\text{Eb}}$ ,
4. the first eccentricity  $\mathbf{e}$ ,
5. the meridian radius of curvature  $M_{\text{E}}$ , and
6. the prime vertical radius of curvature  $N_{\text{E}}$ .

These parameters are either defined (items 1 and 2) or derived (items 3 to 6) based on the WGS 84 (world geodetic system 84, which was originally proposed in 1984 and lastly updated in 2004 [212]) ellipsoid model. More specifically, we have

$$R_{\text{Ea}} = 6,378,137.0 \text{ m}, \quad (2.2)$$

$$\mathbf{f} = 1/298.257223563, \quad (2.3)$$

$$R_{\text{Eb}} = R_{\text{Ea}}(1 - \mathbf{f}) = 6,356,752.0 \text{ m}, \quad (2.4)$$

$$\mathbf{e} = \frac{\sqrt{R_{\text{Ea}}^2 - R_{\text{Eb}}^2}}{R_{\text{Ea}}} = 0.08181919, \quad (2.5)$$

$$M_{\text{E}} = \frac{R_{\text{Ea}}(1 - \mathbf{e}^2)}{(1 - \mathbf{e}^2 \sin^2 \varphi)^{3/2}}, \quad (2.6)$$

$$N_{\text{E}} = \frac{R_{\text{Ea}}}{\sqrt{1 - \mathbf{e}^2 \sin^2 \varphi}}. \quad (2.7)$$

### 2.2.2 Earth-Centered Earth-Fixed Coordinate System

The ECEF coordinate system rotates with the earth around its spin axis. As such, a fixed point on the earth surface has a fixed set of coordinates (see, e.g., [202]). The origin and axes of the ECEF coordinate system (see Fig. 2.1) are defined as follows:

1. The origin (denoted by  $O_e$ ) is located at the center of the earth.
2. The Z-axis (denoted by  $Z_e$ ) is along the spin axis of the earth, pointing to the north pole.
3. The X-axis (denoted by  $X_e$ ) intersects the sphere of the earth at  $0^\circ$  latitude and  $0^\circ$  longitude.
4. The Y-axis (denoted by  $Y_e$ ) is orthogonal to the Z- and X-axes with the usual right-hand rule.

Coordinate vectors expressed in the ECEF frame are denoted with a subscript e. Similar to the geodetic system, the position vector in the ECEF frame is denoted by

$$P_e = \begin{pmatrix} x_e \\ y_e \\ z_e \end{pmatrix}. \quad (2.8)$$

### 2.2.3 Local North-East-Down Coordinate System

The local NED coordinate system is also known as a navigation or ground coordinate system. It is a coordinate frame fixed to the earth's surface. Based on the WGS 84 ellipsoid model, its origin and axes are defined as the following (see also Figs. 2.1 and 2.2):

1. The origin (denoted by  $O_n$ ) is arbitrarily fixed to a point on the earth's surface.
2. The X-axis (denoted by  $X_n$ ) points toward the ellipsoid north (geodetic north).
3. The Y-axis (denoted by  $Y_n$ ) points toward the ellipsoid east (geodetic east).
4. The Z-axis (denoted by  $Z_n$ ) points downward along the ellipsoid normal.

The local NED frame plays a very important role in flight control and navigation. Navigation of small-scale UAV rotorcraft is normally carried out within this frame. Coordinate vectors expressed in the local NED coordinate system are denoted with a subscript n. More specifically, the position vector,  $\mathbf{P}_n$ , the velocity vector,  $\mathbf{V}_n$ , and the acceleration vector,  $\mathbf{a}_n$ , of the NED coordinate system are adopted and are, respectively, defined as

$$\mathbf{P}_n = \begin{pmatrix} x_n \\ y_n \\ z_n \end{pmatrix}, \quad \mathbf{V}_n = \begin{pmatrix} u_n \\ v_n \\ w_n \end{pmatrix}, \quad \mathbf{a}_n = \begin{pmatrix} a_{x,n} \\ a_{y,n} \\ a_{z,n} \end{pmatrix}. \quad (2.9)$$

We also note that in our work, we normally select the takeoff point, which is also the sensor initialization point, in each flight test as the origin of the local NED frame. When it is clear in the context, we also use the following definition throughout the monograph for the position vector in the local NED frame,

$$\mathbf{P}_n = \begin{pmatrix} x \\ y \\ z \end{pmatrix}. \quad (2.10)$$

Furthermore,  $h = -z$  is used to denote the actual height of the unmanned system.

### 2.2.4 Vehicle-Carried North-East-Down Coordinate System

The vehicle-carried NED system is associated with the flying vehicle. Its origin and axes (see Fig. 2.2) are given by the following:

1. The origin (denoted by  $O_{nv}$ ) is located at the center of gravity (CG) of the flying vehicle.
2. The X-axis (denoted by  $X_{nv}$ ) points toward the ellipsoid north (geodetic north).
3. The Y-axis (denoted by  $Y_{nv}$ ) points toward the ellipsoid east (geodetic east).
4. The Z-axis (denoted by  $Z_{nv}$ ) points downward along the ellipsoid normal.

Strictly speaking, the axis directions of the vehicle-carried NED frame vary with respect to the flying-vehicle movement and are thus not aligned with those of the local NED frame. However, as mentioned earlier, the miniature rotorcraft UAVs fly only in a small region with low speed, which results in the directional difference being completely neglectable. As such, it is reasonable to assume that the directions of the vehicle-carried and local NED coordinate systems constantly coincide with each other.

Coordinate vectors expressed in the vehicle-carried NED frame are denoted with a subscript  $nv$ . More specifically, the velocity vector,  $\mathbf{V}_{nv}$ , and the acceleration vector,  $\mathbf{a}_{nv}$ , of the vehicle-carried NED coordinate system are adopted and are, respectively, defined as

$$\mathbf{V}_{nv} = \begin{pmatrix} u_{nv} \\ v_{nv} \\ w_{nv} \end{pmatrix}, \quad \mathbf{a}_{nv} = \begin{pmatrix} a_{x,nv} \\ a_{y,nv} \\ a_{z,nv} \end{pmatrix}. \quad (2.11)$$

### 2.2.5 Body Coordinate System

The body coordinate system is vehicle-carried and is directly defined on the body of the flying vehicle. Its origin and axes (see Fig. 2.2) are given by the following:

1. The origin (denoted by  $O_b$ ) is located at the center of gravity (CG) of the flying vehicle.
2. The X-axis (denoted by  $X_b$ ) points forward, lying in the symmetric plane of the flying vehicle.
3. The Y-axis (denoted by  $Y_b$ ) is starboard (the right side of the flying vehicle).
4. The Z-axis (denoted by  $Z_b$ ) points downward to comply with the right-hand rule.

Coordinate vectors expressed in the body frame are appended with a subscript  $b$ . Next, we define

$$\mathbf{V}_b = \begin{pmatrix} u \\ v \\ w \end{pmatrix} \quad (2.12)$$

to be the vehicle-carried NED velocity, i.e.,  $\mathbf{V}_{nv}$ , projected onto the body frame, and

$$\mathbf{a}_b = \begin{pmatrix} a_x \\ a_y \\ a_z \end{pmatrix} \quad (2.13)$$

to be the vehicle-carried NED acceleration, i.e.,  $\mathbf{a}_{nv}$ , projected onto the body frame. These two vectors are intensively used in capturing the 6-DOF rigid-body dynamics of unmanned systems.

## 2.3 Coordinate Transformations

The transformation relationships among the adopted coordinate frames are introduced in this section. We first briefly introduce some fundamental knowledge related to Cartesian-frame transformations before giving the detailed coordinate transformations.

### 2.3.1 Fundamental Knowledge

We summarize in this subsection the basic concepts of the Euler rotation and rotation matrix, Euler angles, and angular velocity vector used in flight modeling, control and navigation.

#### 2.3.1.1 Euler Rotations

The orientation of one Cartesian coordinate system with respect to another can always be described by three successive Euler rotations [171]. For aerospace application, the Euler rotations perform about each of the three Cartesian axes consequently, following the right-hand rule. Shown in Fig. 2.3 is a simple example, in which Frames C1 and C2 are two Cartesian systems with the aligned Z-axes pointing toward us. We take Frame C2 as the reference and can obtain Frame C1 through a Euler rotation (by rotating Frame C2 counter-clockwise with an angle of  $\xi$ ). Then, it is straightforward to verify that the position vectors of any given point expressed in Frame C1, say  $\mathbf{P}_{C1}$ , and in Frame C2, say  $\mathbf{P}_{C2}$ , are related by

$$\mathbf{P}_{C1} = \mathbf{R}_{C1/C2} \mathbf{P}_{C2}, \quad (2.14)$$

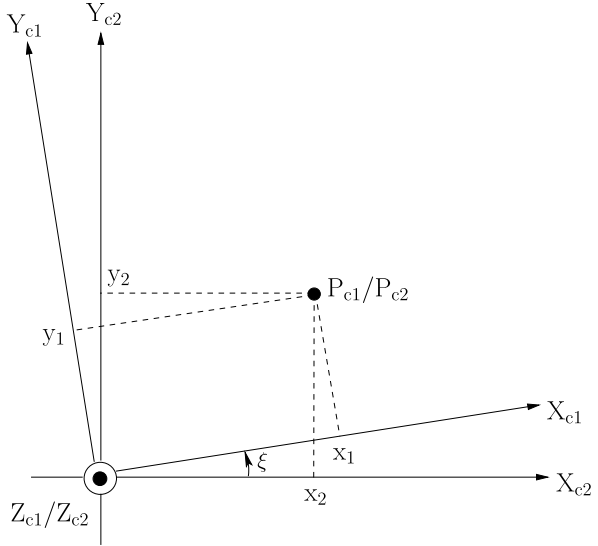
where  $\mathbf{R}_{C1/C2}$  is defined as a rotation matrix that transforms the vector  $\mathbf{P}$  from Frame C2 to Frame C1 and is given as

$$\mathbf{R}_{C1/C2} = \begin{bmatrix} \cos \xi & \sin \xi & 0 \\ -\sin \xi & \cos \xi & 0 \\ 0 & 0 & 1 \end{bmatrix}. \quad (2.15)$$

It is simple to show that

$$\mathbf{R}_{C2/C1} = \mathbf{R}_{C1/C2}^{-1} = \mathbf{R}_{C1/C2}^T. \quad (2.16)$$

**Fig. 2.3** Illustration of a Euler rotation



### 2.3.1.2 Euler Angles

The Euler angles are three angles introduced by Euler to describe the orientation of a rigid body. Although the relative orientation between any two Cartesian frames can be described by Euler angles, we focus in this monograph merely on the transformation between the vehicle-carried (or the local) NED and the body frames, following a particular rotation sequence. More specifically, the adopted Euler angles move the reference frame to the referred frame, following a Z-Y-X (or the so-called 3–2–1) rotation sequence. These three Euler angles are also known as the yaw (or heading), pitch, and roll angles, which are defined as the following (see Fig. 2.4 for graphical illustration):

1. **YAW ANGLE**, denoted by  $\psi$ , is the angle from the vehicle-carried NED X-axis to the projected vector of the body X-axis on the X-Y plane of the vehicle-carried NED frame. The right-handed rotation is about the vehicle-carried NED Z-axis. After this rotation (denoted by  $\mathbf{R}_{\text{int1}/\text{nv}}$ ), the vehicle-carried NED frame transfers to a once-rotated intermediate frame.
2. **PITCH ANGLE**, denoted by  $\theta$ , is the angle from the X-axis of the once-rotated intermediate frame to the body frame X-axis. The right-handed rotation is about the Y-axis of the once-rotated intermediate frame. After this rotation (denoted by  $\mathbf{R}_{\text{int2}/\text{int1}}$ ), we have a twice-rotated intermediate frame whose X-axis coincides with the X-axis of the body frame.
3. **ROLL ANGLE**, denoted by  $\phi$ , is the angle from the Y-axis (or Z-axis) of the twice-rotated intermediate frame to that of the body frame. This right-handed rotation (denoted by  $\mathbf{R}_{\text{b}/\text{int2}}$ ) is about the X-axis of the twice-rotated intermediate frame (or the body frame).

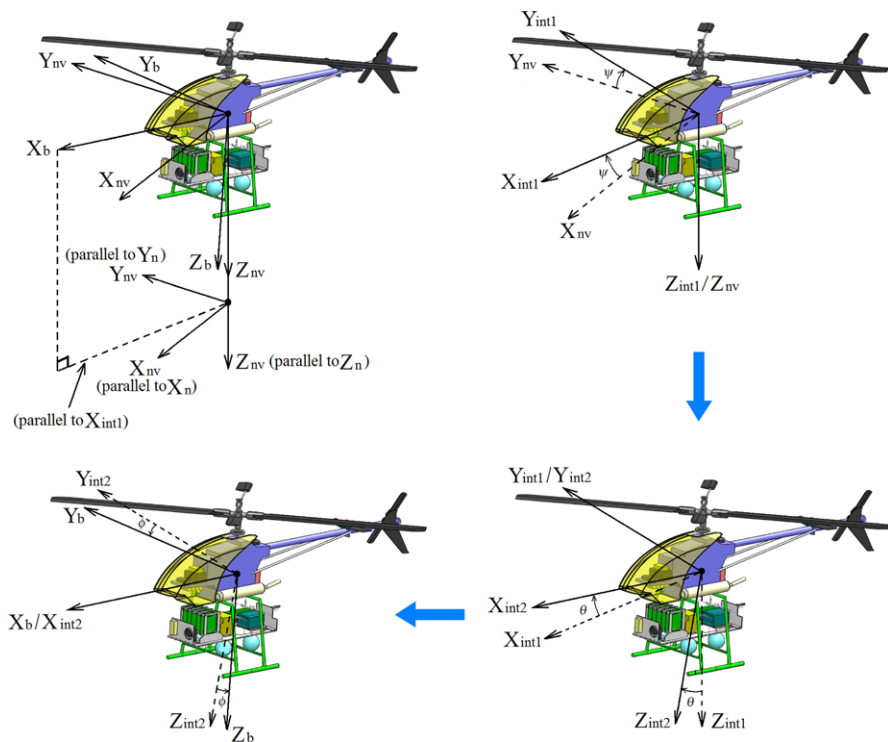


**Fig. 2.4** Euler angles and yaw-pitch-roll rotation sequence

The three relative rotation matrices are respectively given by

$$\mathbf{R}_{int1/nv} = \begin{bmatrix} \cos \psi & \sin \psi & 0 \\ -\sin \psi & \cos \psi & 0 \\ 0 & 0 & 1 \end{bmatrix}, \quad (2.17)$$

$$\mathbf{R}_{int2/int1} = \begin{bmatrix} \cos \theta & 0 & -\sin \theta \\ 0 & 1 & 0 \\ \sin \theta & 0 & \cos \theta \end{bmatrix}, \quad (2.18)$$

and

$$\mathbf{R}_{b/int2} = \begin{bmatrix} 1 & 0 & 0 \\ 0 & \cos \phi & \sin \phi \\ 0 & -\sin \phi & \cos \phi \end{bmatrix}. \quad (2.19)$$



### 2.3.1.3 Angular Velocities

The angular velocities (or angular rates) are associated with the relative motion between two coordinate systems. Considering that Frame C1 is rotating with respect to Frame C2, the angular velocity is denoted by

$$\boldsymbol{\omega}_{C1/C2}^* = \begin{pmatrix} \omega_x \\ \omega_y \\ \omega_z \end{pmatrix}, \quad (2.20)$$

where  $*$  is a coordinate frame on which the angular velocity vector is projected. We note that the coordinate frame  $*$  can be C1 or C2 or any another frame. It is simple to verify that the angular velocity vector of Frame C2 rotating with respect to Frame C1 is given by

$$\boldsymbol{\omega}_{C2/C1}^* = -\boldsymbol{\omega}_{C1/C2}^*. \quad (2.21)$$

## 2.3.2 Coordinate Transformations

We proceed to present the necessary coordinate transformations among the coordinate systems adopted, of which the first three transformations are mainly employed for rotorcraft spatial navigation, the fourth one is commonly adopted for flight control purposes, and finally, the last one focuses on an approximation particularly suitable for the miniature rotorcraft.

### 2.3.2.1 Geodetic and ECEF Coordinate Systems

The position vector transformation from the geodetic system to the ECEF coordinate system is an intermediate step in converting the GPS position measurement to the local NED coordinate system. Given a point in the geodetic system, say

$$P_g = \begin{pmatrix} \lambda \\ \varphi \\ h \end{pmatrix},$$

its coordinate in the ECEF frame is given by

$$\mathbf{P}_e = \begin{pmatrix} x_e \\ y_e \\ z_e \end{pmatrix} = \begin{pmatrix} (N_E + h) \cos \varphi \cos \lambda \\ (N_E + h) \cos \varphi \sin \lambda \\ [N_E(1 - e^2) + h] \sin \varphi \end{pmatrix}, \quad (2.22)$$

where  $e$  and  $N_E$  are as given in (2.5) and (2.7), respectively.

### 2.3.2.2 ECEF and Local NED Coordinate Systems

The position transformation from the ECEF frame to the local NED frame is required together with the transformation from the geodetic system to the ECEF frame

to form a complete position conversion from the geodetic to local NED frames. More specifically, we have

$$\mathbf{P}_n = \mathbf{R}_{n/e}(\mathbf{P}_e - \mathbf{P}_{e,\text{ref}}), \quad (2.23)$$

where  $\mathbf{P}_{e,\text{ref}}$  is the position of the origin of the local NED frame (i.e.,  $\mathbf{O}_n$ , normally the takeoff point in UAV applications) in the ECEF coordinate system, and  $\mathbf{R}_{n/e}$  is the rotation matrix from the ECEF frame to the local NED frame, which is given by

$$\mathbf{R}_{n/e} = \begin{bmatrix} -\sin \varphi_{\text{ref}} \cos \lambda_{\text{ref}} & -\sin \varphi_{\text{ref}} \sin \lambda_{\text{ref}} & \cos \varphi_{\text{ref}} \\ -\sin \lambda_{\text{ref}} & \cos \lambda_{\text{ref}} & 0 \\ -\cos \varphi_{\text{ref}} \cos \lambda_{\text{ref}} & -\cos \varphi_{\text{ref}} \sin \lambda_{\text{ref}} & -\sin \varphi_{\text{ref}} \end{bmatrix}, \quad (2.24)$$

and where  $\lambda_{\text{ref}}$  and  $\varphi_{\text{ref}}$  are the geodetic longitude and latitude corresponding to  $\mathbf{P}_{e,\text{ref}}$ .

### 2.3.2.3 Geodetic and Vehicle-Carried NED Coordinate Systems

In aerospace navigation, a kinematical relationship between geodetic position and vehicle-carried NED velocity is of great importance. The derivative of the geodetic position can be expressed in terms of the vehicle-carried NED velocity as the following:

$$\dot{\lambda} = \frac{v_{\text{nv}}}{(N_E + h) \cos \varphi}, \quad (2.25)$$

$$\dot{\varphi} = \frac{u_{\text{nv}}}{M_E + h}, \quad (2.26)$$

and

$$\dot{h} = -w_{\text{nv}}. \quad (2.27)$$

We note that the first two equations are derived based on spherical triangles, whereas the third one can be easily obtained from the definitions of  $h$  and  $w_{\text{nv}}$ .

The derivatives of the vehicle-carried NED velocities are respectively given by

$$\dot{u}_{\text{nv}} = -\frac{v_{\text{nv}}^2 \sin \varphi}{(N_E + h) \cos \varphi} + \frac{u_{\text{nv}} w_{\text{nv}}}{M_E + h} + a_{\text{mx},\text{nv}}, \quad (2.28)$$

$$\dot{v}_{\text{nv}} = \frac{u_{\text{nv}} v_{\text{nv}} \sin \varphi}{(N_E + h) \cos \varphi} + \frac{v_{\text{nv}} w_{\text{nv}}}{N_E + h} + a_{\text{my},\text{nv}}, \quad (2.29)$$

and

$$\dot{w}_{\text{nv}} = -\frac{v_{\text{nv}}^2}{N_E + h} - \frac{u_{\text{nv}}^2}{M_E + h} + g + a_{\text{mz},\text{nv}}, \quad (2.30)$$

where  $g$  is the gravitational acceleration, and

$$\mathbf{a}_{\text{mea},\text{nv}} = \begin{pmatrix} a_{\text{mx},\text{nv}} \\ a_{\text{my},\text{nv}} \\ a_{\text{mz},\text{nv}} \end{pmatrix} \quad (2.31)$$

is the projection of  $\mathbf{a}_{\text{mea,b}}$ , the proper acceleration measured on the body frame, onto the vehicle-carried NED frame. The proper acceleration is an acceleration relative to a free-fall observer who is momentarily at rest relative to the object being measured [209]. In the above equations, we omit terms related to the earth's self-rotation, which is reasonable for small-scale UAV rotorcraft working in a small confined area.

### 2.3.2.4 Vehicle-Carried NED and Body Coordinate Systems

Kinematical relationships between the vehicle-carried NED and the body frames are important to flight dynamics modeling and automatic flight control. For translational kinematics, we have

$$\mathbf{V}_b = \mathbf{R}_{b/nv} \mathbf{V}_{nv}, \quad (2.32)$$

$$\mathbf{a}_b = \mathbf{R}_{b/nv} \mathbf{a}_{nv}, \quad (2.33)$$

and

$$\mathbf{a}_{\text{mea,b}} = \mathbf{R}_{b/nv} \mathbf{a}_{\text{mea,nv}}, \quad (2.34)$$

where  $\mathbf{R}_{b/nv}$  is the rotation matrix from the vehicle-carried NED frame to the body frame and is given by

$$\mathbf{R}_{b/nv} = \begin{bmatrix} \mathbf{c}_\theta \mathbf{c}_\psi & \mathbf{c}_\theta \mathbf{s}_\psi & -\mathbf{s}_\theta \\ \mathbf{s}_\phi \mathbf{s}_\theta \mathbf{c}_\psi - \mathbf{c}_\phi \mathbf{s}_\psi & \mathbf{s}_\phi \mathbf{s}_\theta \mathbf{s}_\psi + \mathbf{c}_\phi \mathbf{c}_\psi & \mathbf{s}_\phi \mathbf{c}_\theta \\ \mathbf{c}_\phi \mathbf{s}_\theta \mathbf{c}_\psi + \mathbf{s}_\phi \mathbf{s}_\psi & \mathbf{c}_\phi \mathbf{s}_\theta \mathbf{s}_\psi - \mathbf{s}_\phi \mathbf{c}_\psi & \mathbf{c}_\phi \mathbf{c}_\theta \end{bmatrix}, \quad (2.35)$$

and where  $\mathbf{s}_*$  and  $\mathbf{c}_*$  denote  $\sin(*)$  and  $\cos(*)$ , respectively.

For rotational kinematics, we focus on the angular velocity vector  $\boldsymbol{\omega}_{b/nv}^b$ , which describes the rotation of the vehicle-carried NED frame with respect to the body frame projected onto the body frame. Following the definition and sequence of the Euler angles, it can be expressed as

$$\begin{aligned} \boldsymbol{\omega}_{b/nv}^b &:= \begin{pmatrix} p \\ q \\ r \end{pmatrix} = \begin{pmatrix} \dot{\phi} \\ 0 \\ 0 \end{pmatrix} + \mathbf{R}_{b/int2} \left[ \begin{pmatrix} 0 \\ \dot{\theta} \\ 0 \end{pmatrix} + \mathbf{R}_{int2/int1} \begin{pmatrix} 0 \\ 0 \\ \dot{\psi} \end{pmatrix} \right] \\ &= \mathbf{S} \begin{pmatrix} \dot{\phi} \\ \dot{\theta} \\ \dot{\psi} \end{pmatrix}, \end{aligned} \quad (2.36)$$

where  $p$ ,  $q$ , and  $r$  are the standard symbols adopted in the aerospace community for the components of  $\boldsymbol{\omega}_{b/nv}^b$ ,  $\mathbf{R}_{int2/int1}$  and  $\mathbf{R}_{b/int2}$  are respectively given as in (2.18) and (2.19), and lastly,  $\mathbf{S}$  is the lumped transformation matrix given by

$$\mathbf{S} = \begin{bmatrix} 1 & 0 & -\sin \theta \\ 0 & \cos \phi & \sin \phi \cos \theta \\ 0 & -\sin \phi & \cos \phi \cos \theta \end{bmatrix}. \quad (2.37)$$

It is simple to verify that

$$\mathbf{S}^{-1} = \begin{bmatrix} 1 & \sin \phi \tan \theta & \cos \phi \tan \theta \\ 0 & \cos \phi & -\sin \phi \\ 0 & \sin \phi / \cos \theta & \cos \phi / \cos \theta \end{bmatrix}. \quad (2.38)$$

We note that (2.36) is known as the Euler kinematical equation and that  $\theta = \pm 90^\circ$  causes singularity in (2.37), which can be avoided by using quaternion expressions.

### 2.3.2.5 Local and Vehicle-Carried NED Coordinate Frames

As mentioned in Sect. 2.2.4, under the assumption that there is no directional difference between the local and vehicle-carried NED frames, we have

$$\mathbf{V}_n = \mathbf{V}_{nv}, \quad \boldsymbol{\omega}_{b/n}^b = \boldsymbol{\omega}_{b/nv}^b, \quad \mathbf{a}_n = \mathbf{a}_{nv}, \quad \mathbf{a}_{\text{mea},n} = \mathbf{a}_{\text{mea},nv}, \quad (2.39)$$

where  $\mathbf{a}_{\text{mea},n}$  is the projection of the proper acceleration measured on the body frame, i.e.,  $\mathbf{a}_{\text{mea},b}$ , onto the local NED frame. These properties will be used throughout the entire monograph.



<http://www.springer.com/978-0-85729-634-4>

Unmanned Rotorcraft Systems

Cai, G.; Chen, B.M.; Lee, T.H.

2011, XIX, 270 p. 167 illus., 140 illus. in color.,

Hardcover

ISBN: 978-0-85729-634-4